Redox Biology 10 (2016) 233–242

Contents lists available at ScienceDirect

Redox Biology

journal homepage: www.elsevier.com/locate/redox

Hydroxytyrosol inhibits hydrogen peroxide-induced apoptotic signaling via labile iron chelation

Natalia Kitsati, Michalis D. Mantzaris, Dimitrios Galaris*

Laboratory of Biological Chemistry, University of Ioannina, School of Health Sciences, Faculty of Medicine, 451 10 Ioannina, Greece

ARTICLE INFO

Keywords:
Apoptosis
Hydroxytyrosol
Labile iron
Mitogen activated protein kinases
Redox signaling
Tyrosol

ABSTRACT

Although it is known that Mediterranean diet plays an important role in maintaining human health, the underlying molecular mechanisms remain largely unknown. The aim of this investigation was to elucidate the potential role of ortho-dihydroxy group containing natural compounds in H_2O_2-induced DNA damage and apoptosis. For this purpose, the main phenolic alcohols of olive oil, namely hydroxytyrosol and tyrosol, were examined for their ability to protect cultured cells under conditions of oxidative stress. A strong correlation was observed between the ability of hydroxytyrosol to mitigate intracellular labile iron level and the protection offered against H_2O_2-induced DNA damage and apoptosis. On the other hand, tyrosol, which lacks the ortho-dihydroxy group, was ineffective. Moreover, hydroxytyrosol (but not tyrosol), was able to diminish the late sustained phase of H_2O_2-induced JNK and p38 phosphorylation. The derangement of intracellular iron homeostasis, following exposure of cells to H_2O_2, played pivotal role both in the induction of DNA damage and the initiation of apoptotic signaling. The presented results suggest that the protective effects exerted by ortho-dihydroxy group containing dietary compounds against oxidative stress-induced cell damage are linked to their ability to influence changes in the intracellular labile iron homeostasis.

1. Introduction

Accumulating evidence indicates that numerous natural compounds, which are present abundantly in the Mediterranean diet, contribute to the maintenance of human health by preventing oxidative stress-related diseases [1–3]. Regular consumption of olive oil as well as fruits and vegetables is thought to be associated with these health promoting effects and the mode of action of their components have been investigated extensively [4,5].

Apart from a unique source of monounsaturated fatty acids, olive oil also contains different phenolic compounds, such as phenolic acids, phenolic alcohols, flavonoids, secoiridoids and lignans [5,6]. Hydroxytyrosol (3,4-dihydroxyphenylethanol, HTy) and tyrosol (3-hydroxyphenylethanol, Ty) are considered to be the most abundant and representative phenolic alcohols in olive oil [7,8]. These are rather hydrophilic compounds with similar molecular structures, differing only in position 3 of the phenolic ring where the hydrogen atom of Ty is substituted by a hydroxyl group in HTy creating an ortho-dihydroxy moiety (Scheme 1).

It has been suggested that HTy can act as a scavenger of reactive free radicals and in this way protect cells in conditions of oxidative stress [9–12]. Moreover, it can induce the expression of antioxidant enzymes via Nrf2 activation [13–16], reduce expression of cell adhesion molecules [17], inhibit platelet aggregation in rats [18] and exert anti-inflammatory and anti-cancer effects [2,7,19].

We have shown previously that HTy (but not Ty) was able to protect cells in culture from H_2O_2-induced formation of single strand breaks in nuclear DNA [20]. It was also demonstrated, that the ability of several phenolics compounds, including phenolic acids and flavonoids, to protect cells against H_2O_2-induced DNA damage was strongly correlated with their ability to chelate intracellular labile iron [21]. A prerequisite for effective action of a particular compound was its ability to penetrate plasma membrane in order to act in the interior of the cells. Thus, phenolic acids, like caffeic acid, which are negatively charged at neutral pH were largely ineffective, even at relatively high concentrations, although able to chelate iron [22]. On the other hand, their protective capacity was increased when the negatively charged carboxyl group was esterified, thus facilitating their penetration through plasma membrane.

In a recent publication we described also the pivotal role played by intracellular labile iron in redox signaling processes [23]. Thus, it was rational to imagine that dietary components able to modulate intra-

Abbreviations: ERK, extracellular-signal-regulated kinase; FBS, foetal bovine serum; HTy, hydroxytyrosol; JNK, c-Jun NH_2-terminal kinase; MAPK, mitogen activated protein kinase; PI, propidium iodide; PARP-1, poly ADP-ribose polymerase 1; SIH, salicylaldehyde isonicotinoyl hydrazine; Ty, tyrosol

* Corresponding author.
E-mail address: dgalaris@uoi.gr (D. Galaris).

http://dx.doi.org/10.1016/j.redox.2016.10.006
Received 9 September 2016; Received in revised form 3 October 2016; Accepted 11 October 2016
Available online 15 October 2016

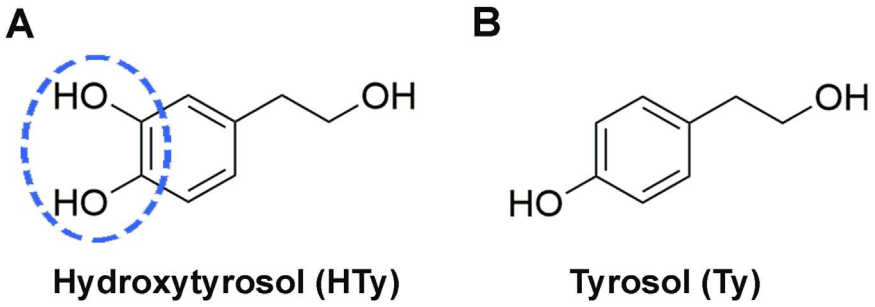

Scheme 1. Chemical structures of the main components of olive oil phenolic fraction, (A) hydroxytyrosol (HTy) and (B) tyrosol (Ty), which were examined in this investigation. The ortho-dihydroxy moiety in HTy is highlighted by the dashed ellipse.

cellular labile iron homeostasis should also influence redox induced signal transduction pathways.

In the present investigation we selected two phenolic alcohols for two particular reasons: (a) they are uncharged, and (b) they differ only in that the one contains the iron-binding ortho-dihydroxy moiety (HTy) while the other (Ty) is devoid of this group. We examined their potential anti-apoptotic capacities under conditions of oxidative stress (exposure to H_2O_2). It was observed that pre-incubation of the cells with HTy (but not Ty) specifically abrogated the H_2O_2-induced elevation of intracellular labile iron level and inhibited the late and sustained phosphorylation phase of JNK and p38 MAP kinases, but did not affect the phosphorylation of ERK. These results underline the potential capacity of diet components which contain the ortho-dihydroxy moiety to modulate intracellular iron homeostasis and in this way to influence redox-mediated signal transduction.

2. Materials and methods

2.1. Materials

RPMI-1640 growth medium, glucose oxidase (G.O.) (from *Aspergillus niger*, 18000 units/g) and tyrosol (79058) were obtained from Sigma-Aldrich Corporation (St. Louis, MO, USA). Fetal bovine serum (FBS), low melting-point agarose and penicillin/streptomycin antibiotics were obtained from Gibco GRL (Grand Island, NY, USA). Normal melting-point agarose was obtained from Serva GmbH (Heidelberg, Germany). Cocktail protease inhibitors were from Roche (Mannheim, Germany). Hydroxytyrosol was purchased from Extra-Synthese (Genay Cedex, France), whereas calcein-AM and propidium iodide (PI) were from Molecular Probes (Eugene, OR, USA). Antibodies used in this study were: anti-ferritin (ab75973) and anti-cytochrome-c (ab133504) from Abcam (Cambridge, MA, USA), anti-PARP-1 (sc-8035), anti-a-Tubulin (TU-02) (sc-7150) and horseradish peroxidase-conjugated secondary antibodies were purchased from Santa Cruz Biotechnology (Santa Cruz, CA, USA), anti-cleaved caspase-3 (#9664), anti-phospho-JNK (#9251S), anti-phosho p38 (#9211), anti-phospho ERK (#9101) and anti-p38 (#9213) from Cell signaling (Danvers, MA, USA), Annexin V–fluorescein isothiocyanate (FITC) was purchased from BD Pharmigen (San Diego, CA, USA). Anti-actin-β (A5441) was obtained from Sigma-Aldrich Corporation (St. Louis, MO, USA). Secondary antibodies anti-rabbit (111-035-144) and anti-mouse (115-035-062) were purchased from Jackson Immunoresearch (Baltimore Pike, West Grove, USA). The specific iron chelator salicylaldehyde isonicotinoyl hydrazone (SIH) was a kind donation from Professor Prem Ponka (McGill University, Montreal, QC, Canada). All other chemicals used were of analytical grade.

2.2. Cell culture

Jurkat cells (ATCC, clone E6-1) was grown in RPMI-1640 containing 10% heat-inactivated FBS, 100 U/ml penicillin, and 100 ng/ml streptomycin, at 37 °C in 95% air, 5% CO_2. Jurkat cells in the log phase were harvested by centrifugation (250*g*, 10 min), resuspended at a density of 1.5×10^6 cells per ml, and allowed to stay for 1 h under standard conditions before treatments.

2.3. Single-cell gel electrophoresis (Comet assay)

The alkaline comet assay was performed as described previously, with minor modifications [24]. In brief, cells were suspended in 1% (w/v) low-melting-point agarose in PBS, pH 7.4, and pipetted onto superfrosted glass microscope slides, precoated with a layer of 1% (w/v) normal melting-point agarose (warmed to 37 °C prior to use). The agarose was allowed to set at 4 °C for 10 min, and the slides were then immersed for 1 h at 4 °C in a lysis solution (2.5 M NaCl, 100 mM EDTA, 10 mM Tris, pH 10, 1% Triton X-100) to dissolve cellular proteins and lipids. Slides were placed in single rows in a 30 cm wide horizontal electrophoresis tank containing 0.3 M NaOH and 1 mM EDTA, pH:~13 (unwinding solution), and kept at 4 °C for 40 min to allow DNA strand separation (alkaline unwinding). Electrophoresis was performed for 30 min in the unwinding solution at 30 V (1 V/cm) and 300 mA. Finally, the slides were washed for 3×5 min in 0.4 M Tris (pH 7.5, 4 °C) and stained with Hoechst 33342 (10 mg/ml).

Hoechst-stained nucleoids were examined under a UV-microscope with a 490 nm excitation filter at a magnification of 400×. DNA damage was not homogeneous, and visual scoring was based on the characterization of 100 randomly selected nucleoids. The comet-like DNA formations were categorized into five classes (0, 1, 2, 3, and 4) representing an increasing extent of DNA damage visualized as a “tail”. Each comet was assigned a value according to its class. Accordingly, the overall score for 100 comets ranged from 0 (100 comets in class 0) to 400 (100 comets in class 4). In this way, the overall DNA damage of the cell population can be expressed in arbitrary units [25]. Scoring expressed in this way correlated linearly with other parameters, such as percentage of DNA in the tail estimated after computer image analysis using a specific software package (Comet Imager; MetaSystems) (results not shown).

2.4. Estimation of intracellular labile iron

Intracellular levels of labile iron were estimated as described by Tenopoulou et al., with minor modifications [26]. Briefly, after the indicated treatments, cells were washed and incubated with 0.15 μm calcein-AM for 15 min at 37 °C in PBS containing 1 mg/ml BSA and 20 mM Hepes, pH 7.3. After calcein loading, cells were washed, resuspended in 2.2 ml of the same buffer without calcein-AM, placed under stirring in a fluorescence spectrophotometer (F-2500; Hitachi) cuvette, and fluorescence was monitored (excitation 488 nm; emission 517 nm). Calcein-loaded cells show a fluorescence component (ΔF) that is quenched after binding to intracellular iron and can be revealed by addition of 90.9 μm SIH, a highly specific and membrane-permeable iron chelator. The increase in fluorescence is analogous to calcein chelated iron. Cell viability (by Trypan Blue exclusion) was > 95% and was unchanged during the assay.

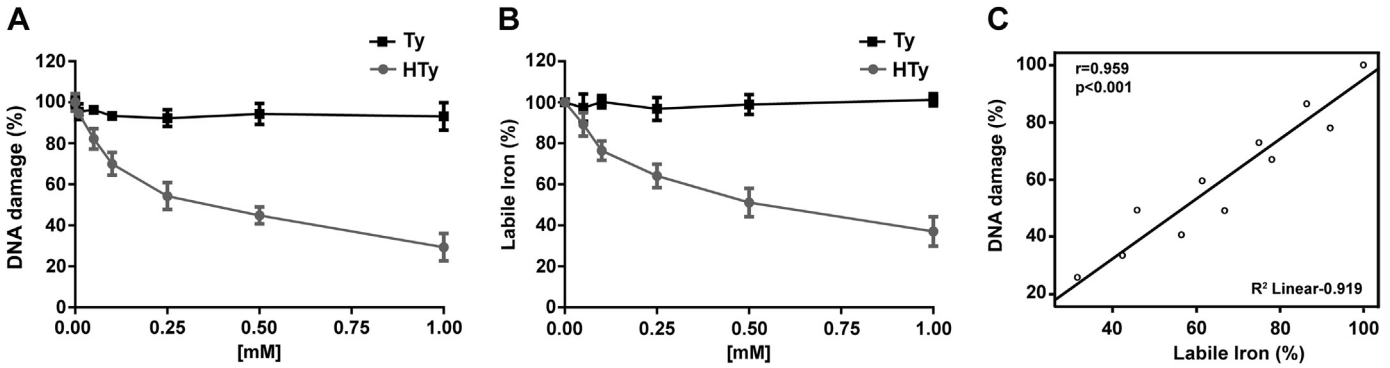

Fig. 1. *Correlation between the protective effect of hydroxytyrosol and its iron binding capacity.* (A) Jurkat cells (1.5×10^6 cells/ml) were incubated for 30 min with the indicated concentrations of HTy (–●–) or (Ty) (-■-) and then exposed for 10 min to 0.6 μg/ml glucose oxidase, able to generate 10 μM H_2O_2 per minute. Formation of single strand breaks in nuclear DNA was estimated by Single Cell Gel Electrophoresis (Comet Assay), as described in "Materials and Methods". The results are expressed as % of DNA damage of control cells exposed to H_2O_2, in the absence of the phenolic compounds. (B) Jurkat cells were incubated with HTy (–●–) or Ty (-■-) for 30 min and the intracellular levels of labile iron were estimated fluorometrically by the calcein method, as describe in "Materials and Methods". Results are expressed as % of labile iron levels of control cells, in the absence of any treatment. (C) Correlation between the protection offered by HTy against H_2O_2-induced DNA damage and its ability to decrease intracellular labile iron (r=0.959, $p < 0.001$).

2.5. Flow cytometry

Jurkat cells were seeded into six-well plates at a density of 3×10^6 cells per well (1.5×10^6 cells/ml) and left for 1 h in the incubation chamber. The cells were then treated with hydroxytyrosol or tyrosol solutions at the indicated concentrations (0.05 mM and 0.1 mM) for 30 min and exposed to a bolus addition of 0.25 mM H_2O_2. After 7 h the cells were collected, centrifuged and cell pellets were suspended in calcium buffer 1×(10 mM Hepes, pH=7.4, 140 mM NaCl, 2.5 mM $CaCl_2$) at a rate 10^5 cells/100 μl. Cells were stained with 5 μl of Annexin V-Fluorescein isothiocynate (FITC) and 5 μl of PI (50 μg/ml) and each sample incubated for 30 min in the dark at room temperature. DNA content was determined on a fluorescence-activated cell sorting flow cytometer (Partec ML, Partec GmbH, Germany).

2.6. Preparation of total and cytosolic extracts

Total cellular protein extracts were prepared by lysing 3×10^6 cells (1.5×10^6 cells/ml) in lysis buffer (50 mM Tris-HCl, pH=7.5, 150 mM NaCl, 1% Triton X-100, 0.5% sodium deoxycholate, 0.1% SDS), 1× cocktail inhibitors of proteases and phosphate inhibitors (2mM sodium orthovanadate, 20mM β-glycerol phosphate and 10mM NaF). The mixture was incubated for 30 min on ice and centrifuged at 14.000×*g* for 30 min at 4 °C. The supernatant was stored for analysis as total cell fraction.

For preparation of cytoplasmic extracts, Jurkat cells (80×10^6 cells/sample) were washed in ice-cold PBS, resuspended in buffer (20 mM Hepes, 10 mM KCl, 1 mM EDTA, 1 mM EGTA, 250 mM sucrose, 1.5 mM $MgCl_2$) and lysed by using a cell craker apparatus (HGM, Heidelberg, Germany). After lysing, cell debris, nuclei and mitochondria were pelleted at 14.000×*g* for 10 min at 4 °C. This supernatant was centrifuged at 100.000×*g* for 1 h at 4 °C and the new supernatant (S-100) was stored at −80 °C and used for analysis as cell cytoplasmic fraction.

2.7. Western blotting

For immmunoblotting analysis, 30–50 μg of protein were loaded with Laemmli Buffer with DTT, separated by SDS-polyacrylamide gel electrophoresis and transferred to nitrocellulose membranes by electroblotting. After blocking with 5% non-fat milk, membranes were incubated with the specific antibodies followed by horseradish peroxidase-conjugated secondary antibody. Membranes were developed using the ECL reagent. Band intensity quantifications were performed by Quantity One (Bio-Rad Laboratories).

2.8. Measurement of hydrogen peroxide generation

The amount of hydrogen peroxide generated by the action of glucose oxidase in PBS containing 5.0 mM glucose was estimated either by following the increase in the absorbance at 240 nm (Molar Extinction Coefficient=43.6 M^{-1} cm^{-1}), or polarographically by using an oxygen electrode (Hansatech Instruments, Norfolk, UK.) detecting the liberation of O_2 following the addition of excess of catalase.

2.9. Protein determination

Protein concentration in the samples was determined by the Bradford method, using bovine serum albumin as a standard.

2.10. Statistical analyses

Results were expressed as the mean ± SEM. Significant differences ($P\leq0.05$) were determined by one-way analysis of variance (ANOVA) followed by Tukey's post hoc test for multiple comparisons between groups. Relationship between two variables was assessed by Spearman's rank correlation coefficient.

3. Results

3.1. The capacity of hydroxytyrosol to decrease intracellular labile iron correlates with its ability to inhibit H_2O_2-induced DNA damage

We have shown previously that HTy and Ty represent main constituents of the polar extracts from olive oil [20]. However, only HTy was able to prevent H_2O_2-induced DNA damage, while Ty was completely ineffective [20,27]. Since the only difference in the chemical structure of the two compounds is the replacement of hydrogen at position 3 in Ty by a hydroxyl group in HTy [Scheme 1], we hypothesised that HTy could exert its protective effects by chelating intracellular labile iron through its ortho-dihydroxy moiety in the same manner as caffeic acid and its analogues did [22]. Indeed, it was observed in the present work that the degree of protection offered by HTy against H_2O_2-induced DNA damage correlated strongly with its ability to decrease the level of intracellular labile iron pool, as it was estimated fluorometrically by the calcein method (r=0.959, $p < 0.001$) (Fig. 1A–C). Ty, like several other phenolic compounds that lack the ortho-dihydroxy moiety, was unable to modulate the level of intracellular labile iron and failed to offer any apparent protection against H_2O_2-induced DNA damage.

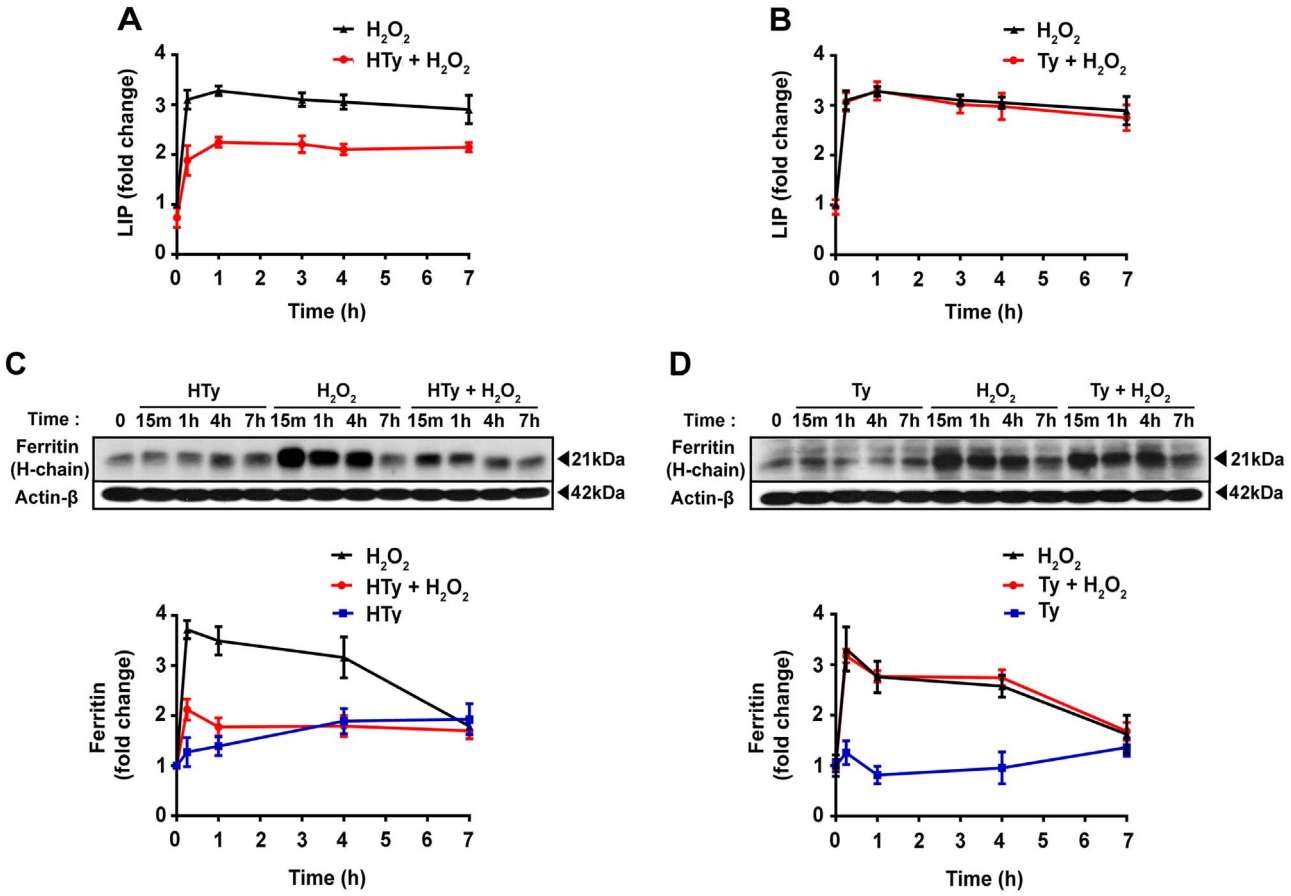

Fig. 2. *Hydroxytyrosol inhibits the elevation of intracellular labile iron after exposure of cells to H_2O_2.* Jurkat cells (1.5×10^6 cells/ml) were preincubated with 50 μm HTy or Ty for 30 min before the addition of 250 μm H_2O_2. (A, B) At the indicated time points, intracellular labile iron levels were monitored by fluorescence analysis using the calcein-AM method, as described in "Materials and Methods". (C, D) Ferritin expression was analyzed by western blot using an antibody that recognized the heavy chain of the protein. Quantification of band intensities is presented in the graphs below (lower panels: black lines=H_2O_2, blue lines=HTy or Ty alone, red lines=H_2O_2 plus HTy or Ty) as the mean ± SEM from three independent experiments, expressed as fold change relative to untreated control cells.

3.2. Hydroxytyrosol attenuates H_2O_2-induced elevation of intracellular labile iron level

It has been reported previously that exposure of Jurkat cells to H_2O_2 provokes a rapid increase of calcein-chelatable intracellular iron that remains elevated for several hours [26,28]. As shown in Fig. 2A, pre-treatment of the cells with 50 μm HTy for 30 min decreased the basal level of cellular labile iron and reduced its H_2O_2-induced elevation. On the other hand, Ty was completely ineffective (Fig. 2B). Surprisingly, the fast rise of H_2O_2-induced elevation of labile iron was accompanied by a rapid and robust induction of the heavy chain of iron storing protein, ferritin (Fig. 2C and D). In this case also, pre-treatment with HTy attenuated the induction of ferritin expression, while Ty failed to do so (Fig. 2C and D). The origin of the detected intracellular labile iron is not known at present. It may be extracellular or mobilized from intracellular sources, which are undetectable by the calcein method [26,29]. However, removal of iron from cell culture medium did not affect the intracellular iron changes induced by H_2O_2 (results not shown), indicating a potential intracellular origin, such as lysosomes, iron-sulfur proteins or ferritin.

3.3. Hydroxytyrosol (but not tyrosol) inhibits H_2O_2-induced and mitochondrial-mediated apoptosis

Next, we tested the capacity of HTy and Ty to protect cells from H_2O_2-induced apoptosis. Exposure of Jurkat cells to bolus addition of 250 μm H_2O_2, increased the percentage of apoptotic cells after 7 h from 7.52 ± 1.73% in the untreated control to 38.06 ± 1.33%, as indicated by Annexin-V binding (Fig. 3). Most apoptotic cells were in early apoptotic phase (32.54 ± 0.96%), as indicated by negative PI staining. Pretreatment of cells with HTy (50 and 100 μm) reduced significantly the number of apoptotic cells to 19.30 ± 0.96% and 21.25 ± 1.65% respectively (*$p < 0.01$ vs H_2O_2-treated cells) (Fig. 3A). On the other hand, pretreatment with Ty was ineffective (Fig. 3B), underlying the potential role of the ortho-dihydroxy moiety of HTy. It has to be noted, that exposure of the cells to 100 μm HTy (but not 100 μm Ty) increased the number of apoptotic cells in the absence of H_2O_2 (7.52 ± 1.73% vs 15.78 ± 3.34%, #$p < 0.01$) (Fig. 3A and B).

In order to further elucidate the underlying molecular mechanism of HTy action, we examined the activation of caspase-3 and the cleavage of the enzyme poly(ADP-ribose) polymerase 1 (PARP-1), which represents one of the substrates for the activated caspase-3. Treatment of cells with 50 μm HTy, 30 min before the exposure of cells to H_2O_2, diminished the cleavage of both caspase-3 and PARP-1 (Fig. 4A), while Ty failed to show any significant inhibitory effect (Fig. 4B). The activation of caspase-3 by H_2O_2 and its prevention by HTy (but not Ty) was also confirmed by measuring the rate of hydrolysis of a specific fluorogenic substrate (peptide Ac-DEVD-AMC) in total cell extracts (results not shown).

The activation of caspase-3 requires the presence of functional "apoptosomes", the formation of which is triggered by the release of cytochrome C from mitochondria to cytosol, following mitochondrial permeability transition. Western blot analysis of cytosolic fractions from Jurkat cells, exposed to 250 μm H_2O_2 for 7 h, showed substantial release of cytochrome C from mitochondria to cytosol (Fig. 5A and B). Again, this release of cytochrome C was reduced significantly when

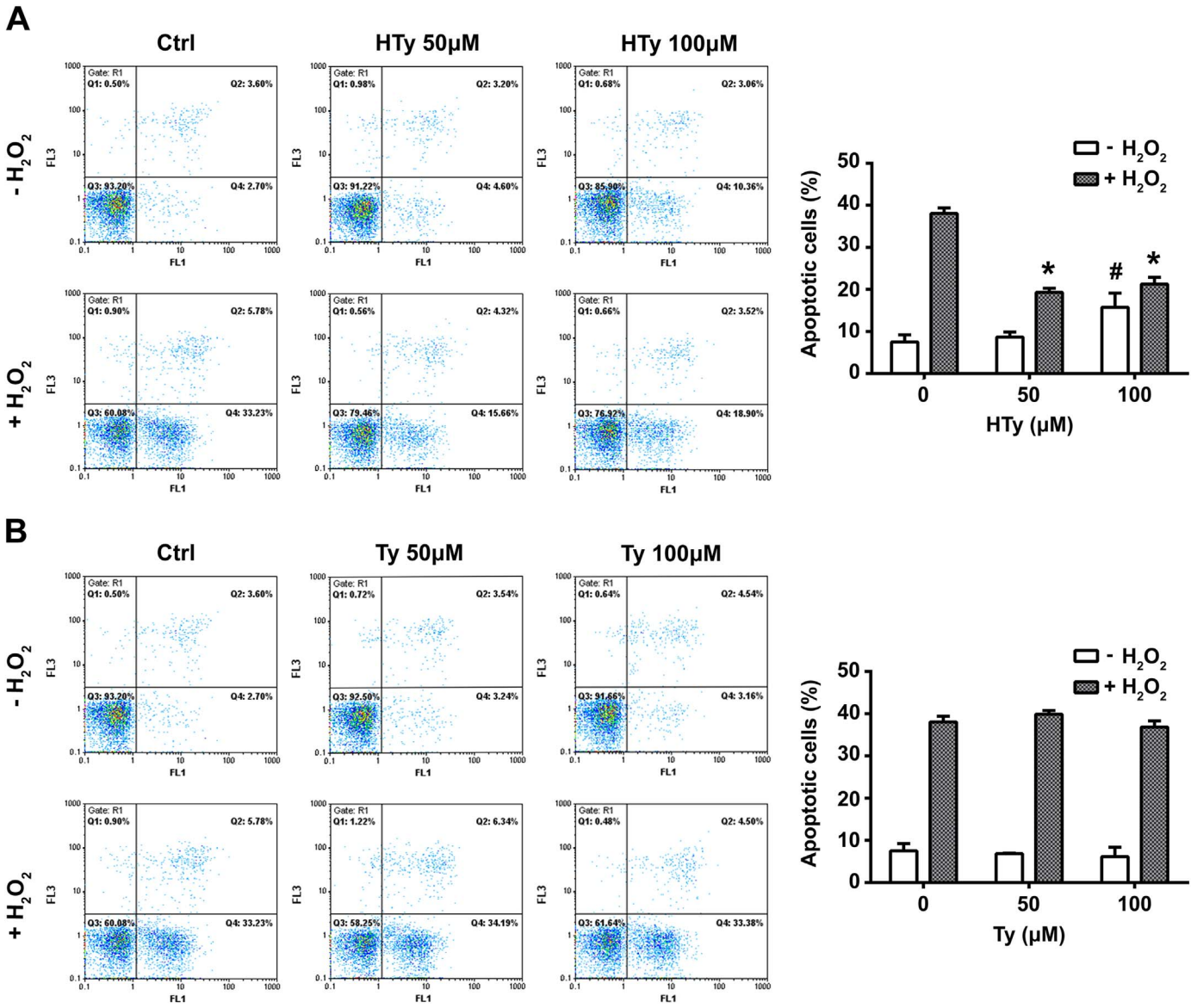

Fig. 3. *Hydroxytyrosol inhibits H_2O_2-induced apoptosis.* Jurkat cells (1.5×10^6 cells/ml) were incubated for 30 min with 50 or 100 μM HTy (A) or Ty (B), before the addition of H_2O_2 (250 μM final concentration). Apoptotic cell death was evaluated 7 h later by flow cytometric analysis of Annexin-V binding cells (horizontal axis) and PI staining (vertical axis). Quantification of apoptotic cells (right side diagrams) was performed by summing the counts of Annexin V-binding cells in Q4 (early apoptotic cells) plus Q2 (late apoptotic cells). Bars represent the mean percentage of Annexin-V positive cells ± SEM from three independent experiments (*$p < 0.01$ vs H_2O_2-treated cells and #$p < 0.01$ vs control untreated cells).

cells were pre-treated with HTy 30 min prior to H_2O_2 addition (Fig. 5A), while pre-treatment with Ty failed to prevent this release (Fig. 5B).

Taken together, the above presented results indicate that HTy inhibits H_2O_2-induced apoptotic cell death by acting at a point on or upstream of mitochondria. Moreover, the fact that Ty failed to prevent apoptosis, under the same circumstances, underlines the obligatory role of the ortho-dihydroxy group in this process.

3.4. Hydroxytyrosol diminishes H_2O_2-induced sustained activation of JNK and p38 MAPKs

It has been proposed previously that sustained phosphorylation of JNK and p38 MAP kinases determine the final fate of cells under conditions of oxidative stress [30]. In order to further investigate the role of HTy in H_2O_2-induced apoptotic signaling, we performed detailed kinetic analysis of the phosphorylation of the main MAP kinases, namely JNK, p38 and ERK. As shown in Fig. 6, exposure of cells to H_2O_2 exerted specific effect on the phosphorylation of MAP kinases. It provoked a robust and sustained phosphorylation of JNK, which culminated at 3–4 h after the addition of H_2O_2, while phosphorylation of p38 showed two characteristic phases, an early and transient at about 5–10 min and a second more extended, which apparently coincided with JNK phosphorylation. On the other hand, the phosphorylation of ERK was rapid, reached the highest level at 30 min and decreased gradually thereafter (Fig. 6A and B). Pre-incubation of the cells for 30 min with HTy inhibited JNK phosphorylation but did not affect significantly ERK phosphorylation (Fig. 6A, lower panel red lines). Interestingly, the same treatment diminished only the second phase of p38, but did not affect the initial short phosphorylation phase (Fig. 6A, lower panel red line). The phosphorylation pattern was not affected in any of the three MAP kinases, when cells were preincubated with Ty (Fig. 6B). Taken together, these observations confirm the involvement JNK/p38 axis in the pathway of H_2O_2-induced apoptotic cell death and demonstrate that the existence of the ortho-dihydroxy group is essential for the HTy molecule in order to exert its modulating effects.

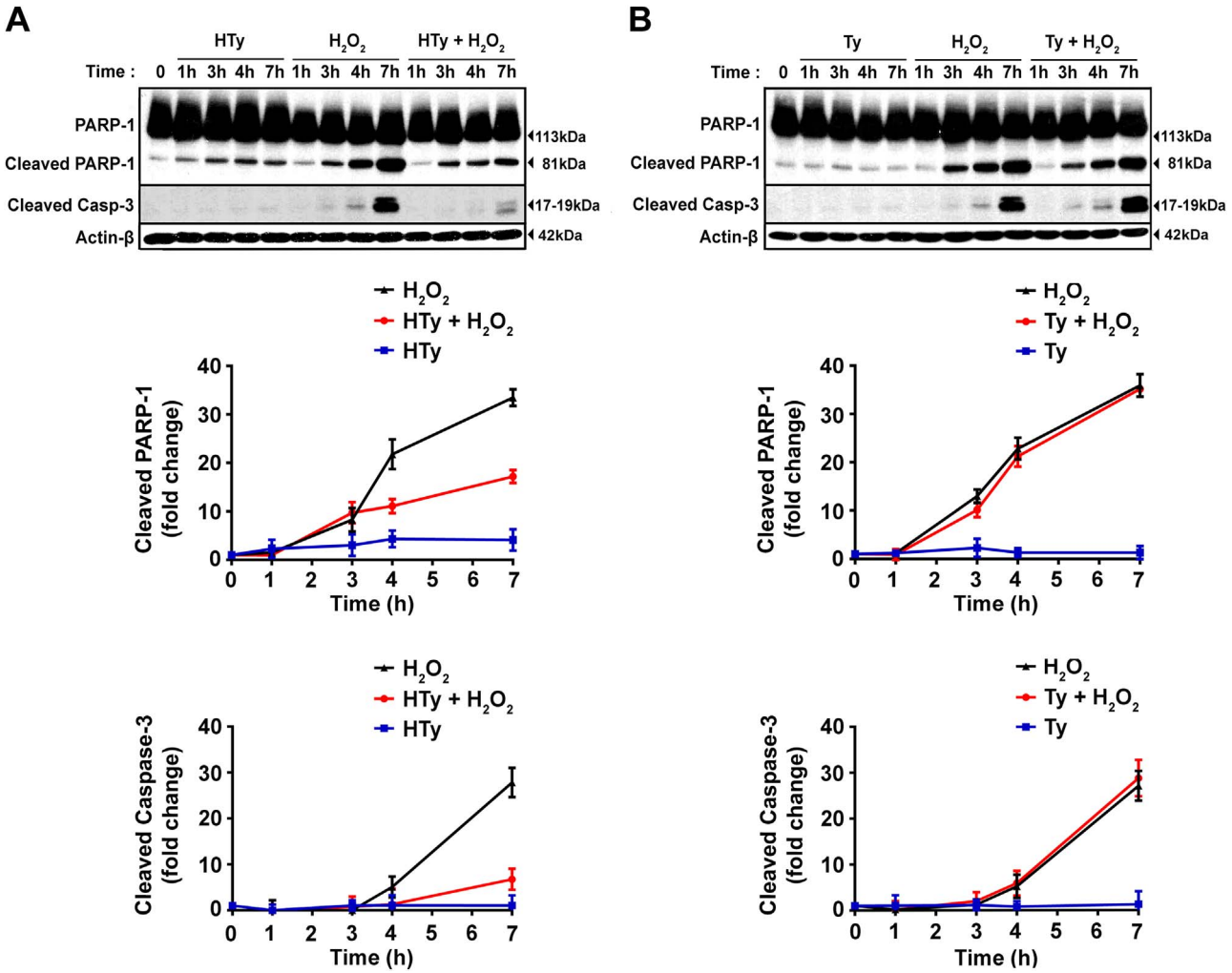

Fig. 4. *Effects of hydroxytyrosol- and tyrosol-treatment on H_2O_2-induced activation of caspase-3 and cleavage of poly(ADP-ribose) polymerase (PARP-1).* Jurkat cells (1.5×10^6 cells/ml) were preincubated with 50 μm HTy (A) or Ty (B) for 30 min before the addition of 250 μm of H_2O_2. At the indicated time points (1, 3, 4 and 7 h), cell extracts were prepared and detection of cleaved caspase-3 and its substrate PARP-1 were evaluated by western blot analysis. Arrow heads at the right indicate the molecular weights for un-cleaved 113 kDa and cleaved 81 kDa parts of PARP-1 and 17–19 kDa of cleaved caspase-3. Quantification of band intensities from (A) and (B) is presented in graphs (lower panels) as the mean ± SEM from three independent experiments expressed as fold change relative to untreated control cells (lines: black=H_2O_2; red=H_2O_2 plus HTy or Ty; blue=HTy or Ty alone).

4. Discussion

The main objective of this study was to examine the potential role of the ortho-dihydroxy structure, which is present abundantly in compounds contained in human diet, in protecting cells from DNA damage and apoptosis induced under conditions of oxidative stress. Moreover, we tested the assumption that the protection offered could be due to the ability of the ortho-dihydroxy group to chelate the intracellular labile iron.

For this purpose, two phenolic alcohols, HTy and Ty, that are abundantly present in olive oil, were used and their protective effects on cells exposed to H_2O_2 were investigated. We selected these particular compounds for three main reasons. Firstly, they represent the main phenolic compounds present in extra virgin olive oil; secondly, in contrast to phenolic acids, phenolic alcohols are not charged and can diffuse easier through cell membranes; and thirdly, they share similar molecular structures, differing only at position 3 of the phenolic ring in Ty, where the hydrogen is replaced by a hydroxyl group in HTy [Scheme 1]. This molecular similarity between the two alcohols allowed us to draw conclusions about the role of the ortho-dihydroxy group, which is also encountered abundantly in many other natural components of human diet and especially in the Mediterranean type of diet. In addition, we tested whether the iron binding capacity of the ortho-dihydroxy structure was able to modulate H_2O_2-induced redox signaling pathways, since previous work from our research group has shown that intracellular labile iron represented an important mediator in H_2O_2-induced apoptotic signaling [23,31,32].

Indeed, it was observed in this study that the presence of the ortho-dihydroxy group in the aromatic ring of HTy provided this molecule with exceptional protective properties against H_2O_2-induced DNA damage and apoptosis. The protective effects were well correlated with the inhibition of H_2O_2-induced changes on intracellular labile iron homeostasis, indicating that iron is apparently implicated in the promotion of sustained phosphorylation and activation of JNK and p38 MAP kinases. Although, we have recently shown that desferrioxamine, a specific iron chelating drug, exerts similar effects on H_2O_2-induced MAP kinase phosporylation pattern [23], according to our knowledge, it is the first time that the patterns of MAPK phosphorylation is linked to intracellular labile iron modulation by the action of specific compounds, which are abundantly present in Mediterranean diet.

4.1. *Hydroxytyrosol inhibits H_2O_2-induced changes in intracellular iron homeostasis*

Intracellular redox-active iron catalyzes the production of highly

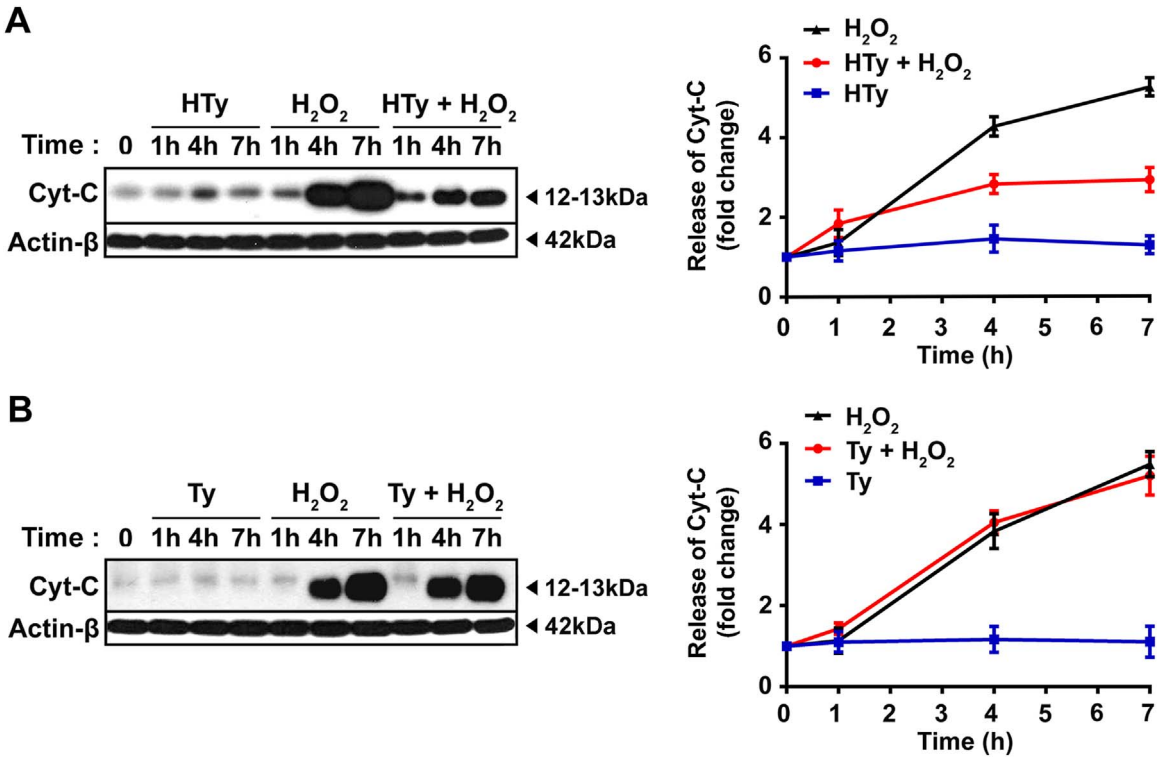

Fig. 5. *Effects of hydroxytyrosol and tyrosol on H_2O_2-induced cytochrome C release from mitochondria to cytosol.* Jurkat cells (1.5×10^6 cells/ml) were preincubated with 50 μm HTy (A) and Ty (B) for 30 min, before the addition of 250 μm of H_2O_2 for the indicated time points. Then, cytosolic fractions were prepared, as described in "Materials and Methods" and analyzed for the presence of cytochrome C by immunoblotting. Quantification of band intensities is presented in graphs at the right side. Values represent the mean ± SEM from three independent experiments, expressed as fold change relative to untreated control cells (lines: black=H_2O_2; red=H_2O_2 plus HTy or Ty; blue=HTy or Ty alone).

toxic hydroxyl radicals, which are able to oxidize indiscriminately all basic cellular components at diffusion controlled rates [33–35]. This redox-active fraction of iron, under normal conditions, comprises only a minor part of total cellular iron and is usually called "labile iron". This iron, however, represents a dynamic pool, the concentration of which can fluctuate in such a way that enables cells to execute distinct cellular functions in an optimal manner according to the prevailing conditions. Thus, under normal conditions the level of labile iron is high enough to just meet the needs for incorporation in newly synthesized proteins, while in conditions of oxidative stress, like those of trauma, infection or inflammation, organisms have developed sophisticated mechanisms to minimize its availability in order to prevent cell toxicity.

The rapid elevation of the acute phase protein ferritin, observed in this work following exposure of cells to H_2O_2 (Fig. 2C and D), ought to be considered as a protective mechanism. It reflects a fast response of cells in order to counteract potential toxic effects arising from the simultaneous presence of increased concentrations of labile iron and H_2O_2. Both H_2O_2-induced labile iron elevation and ferritin expression were diminished in HTy (but not Ty) pre-treated cells (Fig. 2A and C), suggesting the absolute requirement of the ortho-dihyrdoxy group for the effective action. The remarkably fast expression of ferritin presumably indicates that the response was exerted at mRNA stability or mRNA translation levels.

Another question arising from the above results concerns the original source(s) that provided the iron for the observed labile iron elevation following exposure of cells to H_2O_2. Potential intracellular sources are cell organelles, like lysosomes and endoplasmic reticulum as well as proteins, like ferritin and iron-sulfur proteins which contain calcein undetectable iron. Theoretically all these sources may represent targets for H_2O_2 attack and iron release. Obviously, further investigation is needed in order to elucidate this particular point.

4.2. The role of iron in H_2O_2-mediated signaling

Apart from its harmful effects, H_2O_2 has been recently established as indispensable component of specific signal transduction pathways, collectively called "redox signaling" [36,37]. Whether iron is also implicated in these processes is less well examined, although our group has recently presented strong supporting evidence for this notion [23,32]. The main obstacle in explaining the role of iron in H_2O_2-mediated signaling is the difficulty to describe the underlying basic chemistry. It has been established that H_2O_2-signaling proceeds by oxidation of sensitive cysteine residues to sulfenic acid, which represents a two electron oxidation step [38], while the hydroxyl radicals generated after the interaction of H_2O_2 with ferrous iron are one electron oxidants. In order to reconcile this contradiction, we proposed recently that ferryl or perferryl species, which are formed as intermediates during Fenton reaction, could be the actual oxidants in H_2O_2-induced and iron-mediated cysteine oxidations [23].

It was interesting that the observed modulation of H_2O_2-induced MAPK phosphorylation pattern by HTy exerted a high degree of specificity. It diminished the late and sustained phase of JNK and p38 phosphorylation but did not affect the rapidly induced ERK phosphorylation and the early phase of p38 phosphorylation (Fig. 6A). These results predispose for a distinct action of HTy which apparently coincides with the prevention of the elevation of labile iron in the cytosol, following exposure of cells to H_2O_2. Since the actual level of MAPK phosphorylation is determined by the concerted action of upstream MAP2K and MAP3K on one side and the respective MAPK phosphatases on the other, it is plausible to assume that the removal of iron from certain locations in proteins by HTy renders these locations insensitive to oxidation, resulting either to less active upstream kinases or preserving the activity of respective MAPK phosphatases in conditions of oxidative stress. In the absence of HTy (or in the presence of the ineffective Ty), the elevated iron level allows iron ions to be attached on these particular locations, leading to opposite effects.

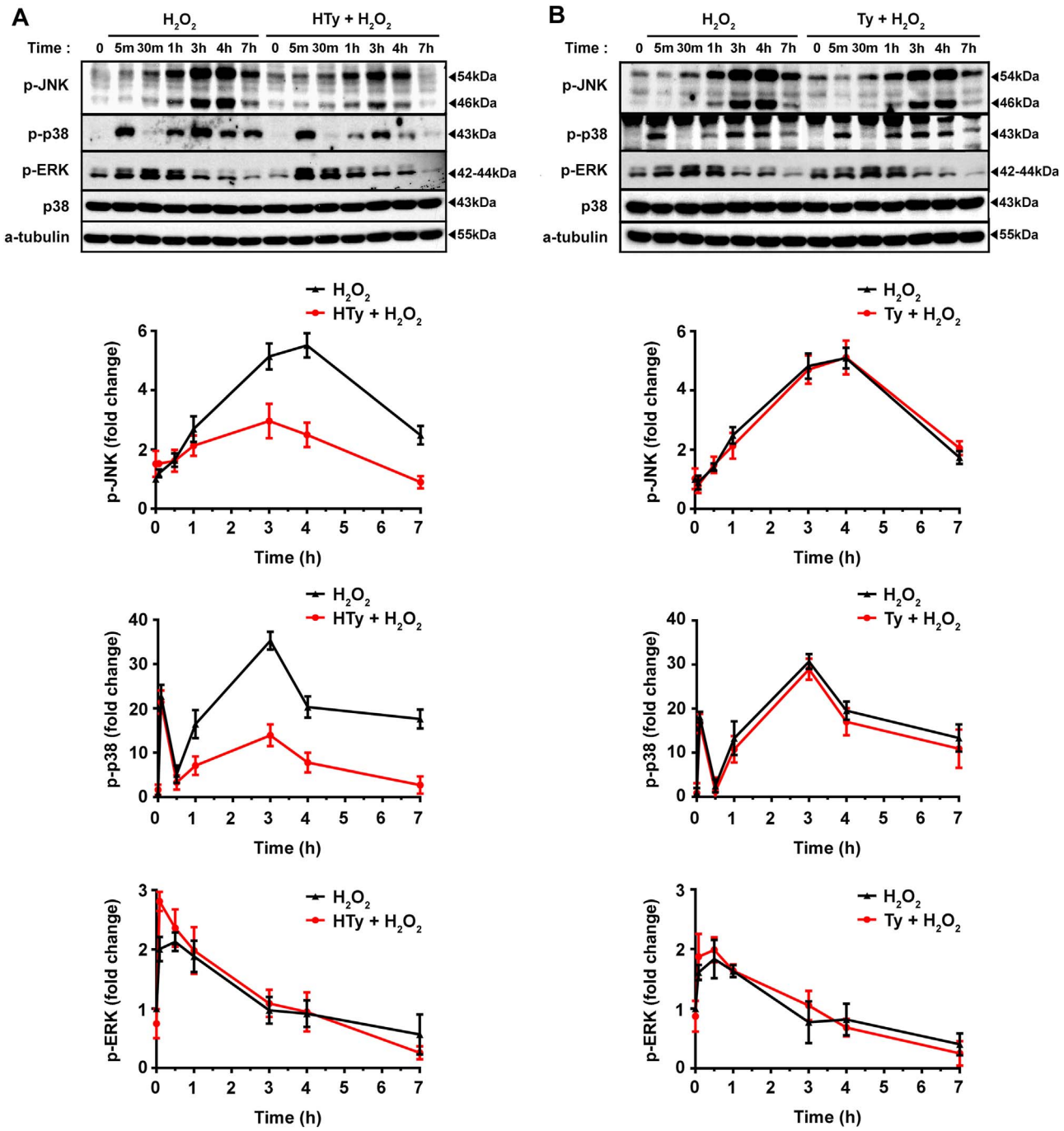

Fig. 6. *Hydroxytyrosol, but not tyrosol, inhibits H_2O_2-induced sustained phosphorylation and activation of the JNK and p38 MAPKs.* Jurkat cells (1.5×10^6 cells/ml) were exposed to 250 μm H_2O_2 for the indicated time points, in the absence or presence of 50 μm HTy (A) or Ty (B), added into the growth medium 30 min before the addition of H_2O_2. At the indicated time points phosphorylation levels of MAP kinases JNK, p38 and ERK were evaluated in total cell extracts by western blot analysis using specific antibodies. Quantification of band intensities for each MAPK is presented in graphs (lower panels) as the mean ± SEM from three independent experiments, expressed as fold change relative to untreated cells (lines: black=H_2O_2; red=H_2O_2 plus HTy or Ty; blue=HTy or Ty alone)..

Whether, iron-mediated activation of upstream MAPKs or inactivation of MAP phosphatases represents the real culprit for the sustained phosphorylation of JNK and p38 MAPKs is not known at present and further investigation is needed to elucidate this mechanism.

4.3. Summary of events taking place following exposure of cells to H_2O_2

The consecutive steps that are proposed to take place, following exposure of cultured cells to H_2O_2 and the mode of action of HTy, are depicted schematically in Fig. 7. (1) A gradient of H_2O_2 concentration is formed between the extracellular and the intracellular space [39]. (2) Within cells, H_2O_2 is reduced to H_2O mainly by the enzymes peroxiredoxin (Prx) and glutathione peroxidase (GPx). As the amount of added H_2O_2 increases, its removal by the cells lasts longer, allowing it to interact with less sensitive targets inside the cells. (3) The presence of H_2O_2 inside the cells provokes a substantial elevation of calcein-chelatable labile iron (Fig. 2). (4) The elevation of intracellular labile iron is associated with specific robust and prolonged phosphorylation of JNK and p38 MAPKs, following exposure of cells to H_2O_2. (5) The induction of ERK phosphorylation and the first phase of p38 phosphorylation are iron-independent processes. (6) In the presence of

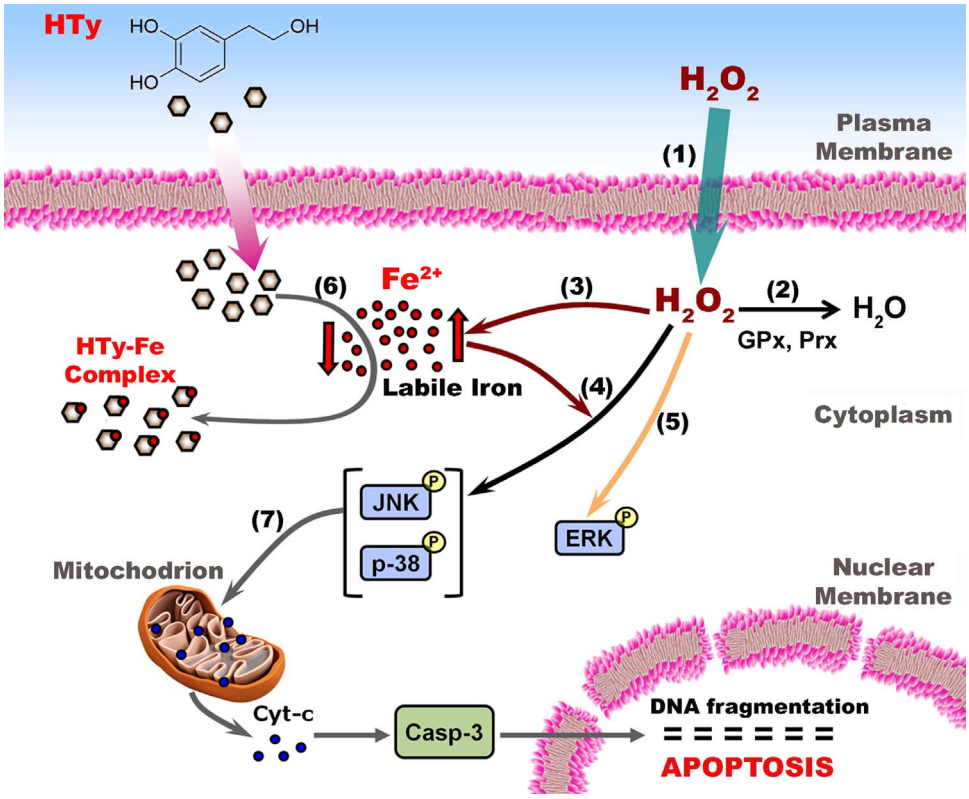

Fig. 7. *Schematic representation of events taking place following exposure of cells to H_2O_2. in the presence of HTy.* Exogenous H_2O_2 can penetrate easily the plasma membrane and reaches the cytosolic compartment (point 1). In cytosol, H_2O_2 is reduced to H_2O by the enzymes GPx and Prx (point 2). However, when the intracellular concentration of H_2O_2 is elevated, it provokes the increase of cytosolic labile iron level (point 3), a fact that facilitates the sustained phosphorylation of MAP kinases JNK and p38 (point 4). H_2O_2 induces also the phosphorylation of ERK, but this event is iron independent (point 5). In the presence of iron-chelating compounds, like HTy, the labile iron level is reduced (point 6), thus, attenuating the H_2O_2-induced and labile iron-mediated prolonged phosphorylation of JNK and p38. Sustained phosphorylation of JNK and p38 leads ultimately to mitochondrial destabilization (point 7), followed by cytochrome C release, caspase 3 activation and cell apoptosis..

HTy, the nature of intracellular labile iron is modulated due to its removal from distinct locations through the chelating action of the ortho-dihydroxy group of this compound, inhibiting labile iron-dependent activation of JNK and p38 MAPKs. (7) Robust and prolonged activation of the JNK and p38 MAPKs induces mitochondrial permeability changes that ultimately culminate to cell apoptosis.

Based on the results presented in this work, it is proposed that any compound contained in human diet that can penetrate through biological membranes and, in addition, is able to chelate intracellular labile iron is likely to abrogate H_2O_2-induced DNA damage and apoptotic redox signaling. Although, in *in vivo* conditions it is unlikely to reach the intracellular levels of HTy used in this study due to biodistribution processes and xenobiotic metabolism, it is plausible to assume that the combined effect of a plethora of iron-binding compounds present in phenolic-rich diets could act additively in modulating intracellular labile iron homeostasis and in this way protect cells under oxidative stress conditions.

Since redox signaling is involved in diverse pathological conditions, the elucidation of the role of iron in these mechanisms represents a main challenge in the field of redox biology. Better understanding of the underlying molecular mechanisms should provide the basis for development of novel strategies to prevent or treat serious diseases linked to oxidative stress [40].

Conflicts of interest

The authors declare that they have no competing interests.

Acknowledgements

This research did not receive any specific grant from funding agencies in the public, commercial, or not-for-profit sectors.

References

[1] A. Trichopoulou, T. Costacou, C. Bamia, D. Trichopoulos, Adherence to a Mediterranean diet and survival in a Greek population, N. Engl. J. Med. 348 (2003) 2599–2608.
[2] E. Scoditti, N. Calabriso, M. Massaro, M. Pellegrino, C. Storelli, G. Martines, R. De Caterina, M.A. Carluccio, Mediterranean diet polyphenols reduce inflammatory angiogenesis through MMP-9 and COX-2 inhibition in human vascular endothelial cells: a potentially protective mechanism in atherosclerotic vascular disease and cancer, Arch. Biochem. Biophys. 527 (2012) 81–89.
[3] J. Shen, K.A. Wilmot, N. Ghasemzadeh, D.L. Molloy, G. Burkman, G. Mekonnen, M.C. Gongora, A.A. Quyyumi, L.S. Sperling, Mediterranean dietary patterns and cardiovascular health, Annu. Rev. Nutr. 35 (2015) 425–449.
[4] G. Buckland, C.A. Gonzalez, The role of olive oil in disease prevention: a focus on the recent epidemiological evidence from cohort studies and dietary intervention trials, Br. J. Nutr. 113 (Suppl 2) (2015) S94–S101.
[5] J. Rodriguez-Morato, L. Xicota, M. Fito, M. Farre, M. Dierssen, R. de la Torre, Potential role of olive oil phenolic compounds in the prevention of neurodegenerative diseases, Molecules 20 (2015) 4655–4680.
[6] C. Romero, M. Brenes, Analysis of total contents of hydroxytyrosol and tyrosol in olive oils, J. Agric. Food Chem. 60 (2012) 9017–9022.
[7] S. Granados-Principal, J.L. Quiles, C.L. Ramirez-Tortosa, P. Sanchez-Rovira, M.C. Ramirez-Tortosa, Hydroxytyrosol: from laboratory investigations to future clinical trials, Nutr. Rev. 68 (2010) 191–206.
[8] G. Blekas, C. Vassilakis, C. Harizanis, M. Tsimidou, D.G. Boskou, Biophenols in table olives, J. Agric. Food Chem. 50 (2002) 3688–3692.
[9] T. Hashimoto, M. Ibi, K. Matsuno, S. Nakashima, T. Tanigawa, T. Yoshikawa, C. Yabe-Nishimura, An endogenous metabolite of dopamine, 3,4-dihydroxyphenylethanol, acts as a unique cytoprotective agent against oxidative stress-induced injury, Free Radic. Biol. Med. 36 (2004) 555–564.
[10] S.J. Rietjens, A. Bast, G.R. Haenen, New insights into controversies on the antioxidant potential of the olive oil antioxidant hydroxytyrosol, J. Agric. Food Chem. 55 (2007) 7609–7614.
[11] L. Goya, R. Mateos, L. Bravo, Effect of the olive oil phenol hydroxytyrosol on human hepatoma HepG2 cells. Protection against oxidative stress induced by *tert*-butylhydroperoxide, Eur. J. Nutr. 46 (2007) 70–78.
[12] S. Schaffer, W.E. Muller, G.P. Eckert, Cytoprotective effects of olive mill wastewater

extract and its main constituent hydroxytyrosol in PC12 cells, Pharmacol. Res. 62 (2010) 322–327.
[13] T. Nguyen, C.S. Yang, C.B. Pickett, The pathways and molecular mechanisms regulating Nrf2 activation in response to chemical stress, Free Radic. Biol. Med. 37 (2004) 433–441.
[14] M.A. Martin, S. Ramos, A.B. Granado-Serrano, I. Rodriguez-Ramiro, M. Trujillo, L. Bravo, L. Goya, Hydroxytyrosol induces antioxidant/detoxificant enzymes and Nrf2 translocation via extracellular regulated kinases and phosphatidylinositol-3-kinase/protein kinase B pathways in HepG2 cells, Mol. Nutr. Food Res 54 (2010) 956–966.
[15] H. Zrelli, M. Matsuoka, S. Kitazaki, M. Araki, M. Kusunoki, M. Zarrouk, H. Miyazaki, Hydroxytyrosol induces proliferation and cytoprotection against oxidative injury in vascular endothelial cells: role of Nrf2 activation and HO-1 induction, J. Agric. Food Chem. 59 (2011) 4473–4482.
[16] X. Zou, Z. Feng, Y. Li, Y. Wang, K. Wertz, P. Weber, Y. Fu, J. Liu, Stimulation of GSH synthesis to prevent oxidative stress-induced apoptosis by hydroxytyrosol in human retinal pigment epithelial cells: activation of Nrf2 and JNK-p62/SQSTM1 pathways, J. Nutr. Biochem 23 (2012) 994–1006.
[17] M.A. Carluccio, M.A. Ancora, M. Massaro, M. Carluccio, E. Scoditti, A. Distante, C. Storelli, R. De Caterina, Homocysteine induces VCAM-1 gene expression through NF-kappaB and NAD(P)H oxidase activation: protective role of Mediterranean diet polyphenolic antioxidants, Am. J. Physiol. Heart Circ. Physiol. 293 (2007) H2344–H2354.
[18] J.A. Gonzalez-Correa, M.D. Navas, J.A. Lopez-Villodres, M. Trujillo, J.L. Espartero, J.P. De La Cruz, Neuroprotective effect of hydroxytyrosol and hydroxytyrosol acetate in rat brain slices subjected to hypoxia-reoxygenation, Neurosci. Lett. 446 (2008) 143–146.
[19] C. Manna, V. Migliardi, F. Sannino, A. De Martino, R. Capasso, Protective effects of synthetic hydroxytyrosol acetyl derivatives against oxidative stress in human cells, J. Agric. Food Chem. 53 (2005) 9602–9607.
[20] L. Nousis, P.T. Doulias, N. Aligiannis, D. Bazios, A. Agalias, D. Galaris, S. Mitakou, DNA protecting and genotoxic effects of olive oil related components in cells exposed to hydrogen peroxide, Free Radic. Res. 39 (2005) 787–795.
[21] M. Melidou, K. Riganakos, D. Galaris, Protection against nuclear DNA damage offered by flavonoids in cells exposed to hydrogen peroxide: the role of iron chelation, Free Radic. Biol. Med. 39 (2005) 1591–1600.
[22] N. Kitsati, D. Fokas, M.D. Ouzouni, M.D. Mantzaris, A. Barbouti, D. Galaris, Lipophilic caffeic acid derivatives protect cells against H2O2-Induced DNA damage by chelating intracellular labile iron, J. Agric. Food Chem. 60 (2012) 7873–7879.
[23] M.D. Mantzaris, S. Bellou, V. Skiada, N. Kitsati, T. Fotsis, D. Galaris, Intracellular labile iron determines H2O2-induced apoptotic signaling via sustained activation of ASK1/JNK-p38 axis, Free Radic. Biol. Med. 97 (2016) 454–465.
[24] N.P. Singh, M.T. McCoy, R.R. Tice, E.L. Schneider, A simple technique for quantitation of low levels of DNA damage in individual cells, Exp. Cell Res. 175 (1988) 184–191.
[25] M. Panayiotidis, O. Tsolas, D. Galaris, Glucose oxidase-produced H2O2 induces Ca2+-dependent DNA damage in human peripheral blood lymphocytes, Free Radic. Biol. Med. 26 (1999) 548–556.
[26] M. Tenopoulou, P.T. Doulias, A. Barbouti, U. Brunk, D. Galaris, Role of compartmentalized redox-active iron in hydrogen peroxide-induced DNA damage and apoptosis, Biochem. J. 387 (2005) 703–710.
[27] A. Barbouti, E. Briasoulis, D. Galaris, Protective Effects of Olive Oil Components Against Hydrogen Peroxide-induced DNA Damage: The Potential Role of Iron Chelation, in: V.R. Preedy, R.R. Watson (Eds.), Olives and olive oil in health and disease prevention, Academic Press, Oxford, 2010, pp. 1103–1109.
[28] A. Al-Qenaei, A. Yiakouvaki, O. Reelfs, P. Santambrogio, S. Levi, N.D. Hall, R.M. Tyrrell, C. Pourzand, Role of intracellular labile iron, ferritin, and antioxidant defence in resistance of chronically adapted Jurkat T cells to hydrogen peroxide, Free Radic. Biol. Med. 68 (2014) 87–100.
[29] M. Tenopoulou, T. Kurz, P.T. Doulias, D. Galaris, U.T. Brunk, Does the calcein-AM method assay the total cellular 'labile iron pool' or only a fraction of it?, Biochem. J. 403 (2007) 261–266.
[30] H. Ichijo, E. Nishida, K. Irie, P. ten Dijke, M. Saitoh, T. Moriguchi, M. Takagi, K. Matsumoto, K. Miyazono, Y. Gotoh, Induction of apoptosis by ASK1, a mammalian MAPKKK that activates SAPK/JNK and p38 signaling pathways, Science 275 (1997) 90–94.
[31] P.T. Doulias, S. Christoforidis, U.T. Brunk, D. Galaris, Endosomal and lysosomal effects of desferrioxamine: protection of HeLa cells from hydrogen peroxide-induced DNA damage and induction of cell-cycle arrest, Free Radic. Biol. Med. 35 (2003) 719–728.
[32] A. Barbouti, C. Amorgianiotis, E. Kolettas, P. Kanavaros, D. Galaris, Hydrogen peroxide inhibits caspase-dependent apoptosis by inactivating procaspase-9 in an iron-dependent manner, Free Radic. Biol. Med. 43 (2007) 1377–1387.
[33] E.D. Weinberg, The hazards of iron loading, Metallomics 2 (2010) 732–740.
[34] D. Galaris, K. Pantopoulos, Oxidative stress and iron homeostasis: mechanistic and health aspects, Crit. Rev. Clin. Lab. Sci. 45 (2008) 1–23.
[35] E. Cadenas, Biochemistry of oxygen toxicity, Annu. Rev. Biochem. 58 (1989) 79–110.
[36] H.S. Marinho, C. Real, L. Cyrne, H. Soares, F. Antunes, Hydrogen peroxide sensing, signaling and regulation of transcription factors, Redox Biol. 2 (2014) 535–562.
[37] L.E. Netto, F. Antunes, The roles of peroxiredoxin and thioredoxin in hydrogen peroxide sensing and in signal transduction, Mol. Cells 39 (2016) 65–71.
[38] G. Roos, J. Messens, Protein sulfenic acid formation: from cellular damage to redox regulation, Free Radic. Biol. Med. 51 (2011) 314–326.
[39] F. Antunes, E. Cadenas, Estimation of H2O2 gradients across biomembranes, FEBS Lett. 475 (2000) 121–126.
[40] D.P. Jones, Redefining oxidative stress, Antioxid. Redox Signal. 8 (2006) 1865–1879.